EURASIAN PHYSICAL TECHNICAL JOURNAL

2026, Volume 23, No. 1(55)

https://doi.org/10.31489/2026N1/101-112

Received: 22/01/2026 Revised: 05/02/2026 Accepted: 19/03/2026 Published online: 30/03/2026

Research Article

UDC 536.24, 004.94

MODELING OF HEAT TRANSFER AND HYDRODYNAMICS OF WATER-OIL HEAT CARRIERS IN HEAT EXCHANGERS

Zhumanbayeva A.S.[1], Volkov K.N.[2]*, Jaichibekov N.Zh.[1], Kurmanova D.E.[1]

[1] L.N. Gumilyov Eurasian National University, Astana, Kazakhstan
[2] Kingston University, London SW15 3DW, UK
Correspondence: jas968@mail.ru

Abstract. *Increased energy efficiency in the extraction and transportation of highly viscous oil is achieved by reducing its viscosity through heating. Numerical modeling is a powerful tool for developing and analyzing methods to improve heat transfer efficiency and optimize the design of heat exchange devices in the oil and gas industry. To solve this problem, the study uses Reynolds-averaged Navier-Stokes equations supplemented with turbulence models (k–ε, k–ω SST, and Transition SST) capable of accounting for the transition from laminar flow to turbulent flow with variable viscosity. The results of calculations of smooth and spiral pipes are compared, as well as an assessment of the reliability and performance of turbulence models used to simulate the operation of heat exchangers with direct and reverse heat flow. The dependences of the numbers Nu and Re of the oil flow in a washed by water pipe for all three turbulence models are shown in comparison with the corresponding experimental result, indicating the qualitative agreement of the numerical calculation results with the experiment. The results of the comparative analysis showed that the kw SST model most effectively describes the flow movement in the inter-tube space. The Computational Fluid Dynamics calculation data obtained is of practical importance for the design and optimization of heat exchanger structures.*

Keywords: heat exchanger, heat exchange, turbulence, modeling, intensification, helicoid tube, oil, hydrodynamics, laminar-turbulent transition, viscosity

1. Introduction

The efficiency of high-speed heat exchangers is achieved due to the intensification of heat exchange, which is provided by swirling the coolant flows. This vortex movement radically changes the hydrodynamics of currents: it increases their kinetic energy, causes severe turbulence and intense mixing of layers, which together significantly improves heat transfer performance. In addition, the vortex motion reduces the hydraulic resistance of the device and promotes self-cleaning of heating surfaces from hardened deposits. The twisting of the medium in the intertubular space is provided by the spiral seams of the housing, which, in addition to their main function, also act as stiffeners. This method of reinforcing the structure is innovative, since traditionally, the thickness of their walls is increased to increase the strength of heat exchangers.

In [1, 2] modeling and calculation of the hydrodynamics of heat carriers (water, oil) flowing through smooth pipes were carried out. In these works, empirical formulas were used for heat transfer from [3]. The information gathered during numerical modeling is used to determine the best approaches for heat transfer intensification [4, 5]. Research indicates that the viscosity of oil has less of an impact on the pipeline's hydraulic properties when it is transported in highly turbulent conditions.

The curvature of the pipe has a significant effect on heat transfer and flow hydrodynamics [6]. In [7], the characteristics of a helicoid tube's movement and heat exchange in heat exchangers of various shapes with straight-tube heat exchangers under different operating conditions were compared. A wide range of studies on increasing the heat transfer rate and reducing the size and cost of shell-and-tube heat exchangers is presented in [8]. Artificial roughness using a corrugated surface improves heat transfer characteristics by destroying and destabilizing the thermal boundary layer.

The coefficient of convective heat transfer in both helicoid and direct tubular heat exchangers under turbulent flow conditions was experimentally determined in [9]. The overall heat transfer coefficient in helicoid heat exchangers is much higher than in straight tube heat exchangers. Helical fins provide higher heat transfer speeds and efficiency than straight pipes due to the development of secondary flow inside the helicoid tube [10]. In [11], an analysis of a spiral-wound heat exchanger was carried out taking into account various boundary conditions. Setting the boundary conditions of constant temperature or constant heat flow for a real heat exchanger does not lead to agreement between the calculated and experimental data. To improve the accuracy of calculations, it is necessary to take into account the coupled heat transfer. Studies of the characteristics of a spiral tubular heat exchanger with different inner tube geometries have been devoted to [12, 13]. [14] presents a numerical study of the characteristics of heat transfer and pressure losses in a vortex cooling pipe with five tangential inlet nozzles and recesses on the inner surface of the pipe. The recesses on the inner surface of the pipe lead to an intensification of heat transfer (the heat transfer coefficient increases by 7.2%) due to the increased heat transfer area and the interaction between the swirling flow and the wall with recesses. A numerical study of heat transfer and entropy generation during laminar flow in screw tubes of various cross-sections is considered in [15].

By facilitating and sealing the tube bundle in support elements made of polymer materials, the maximum possible heat exchange surface is achieved in high-speed heat exchangers [16, 17]. The dynamics of fluid flow in the inter-tube space of heat exchangers is characterized by a high degree of complexity and is influenced by many factors. Heating of oil and petroleum products is a widely used method to reduce energy losses during their transportation [18]. Numerical modeling of heat exchange processes in heat exchange devices with various designs is presented in [19]. The results of the conducted studies indicate a decrease in the influence of the viscosity of the pumped oil on the hydraulic characteristics of the pipeline system under developed flow turbulence conditions. The movement of liquid in the inter-tube space of heat exchangers is highly complex and is due to a number of factors. Heating of oil and petroleum products is actively used to minimize energy losses during their transportation [18]. Numerical modeling of heat exchange processes in apparatuses of different configurations is considered in the source [19]. The data obtained indicate that with the developed turbulence of the flow, the influence of the viscosity of the transported oil on the hydraulic parameters of the pipeline is significantly weakened. A comparative analysis of the accuracy of various turbulence models used to solve the Reynolds equations, the dynamics of heat and mass transfer processes is the object of research in the works [20-26]. In computational practice the three turbulent models are typically employed. A sufficient agreement between the outcomes of numerical modeling and the data collected during industrial tests can be achieved through calculations carried out utilizing these models [2].

The present study presents the results of numerical modeling analyzing the flow and heat transfer in helicoid-shaped pipes. These data are compared with similar indicators for smooth pipes. During the calculations, parameters such as the degree of pipe twist, flow rate, and initial oil temperature were varied. Special attention is paid to how the geometry of a spiral tube affects hydrodynamics and heat transfer, in particular, flow turbulence and its role in increasing heat transfer efficiency. Various approaches have been used to model turbulence, including the k–ε, k–ω *SST*, and Transition *SST* models (which take into account the laminar-turbulent transition). Comparing the results of these models with data from physical experiments and semi-empirical calculations allows us to determine the most suitable turbulence model for designing direct-flow and countercurrent heat exchangers.

2. Model and calculation method

Method of modeling and computation The Navier-Stokes equations modified by Reynolds (RANS) are used for numerical simulation of hydrodynamics and thermal transfer of an incompressible fluid with changing viscosity. The three turbulence models, which takes the luminaire-turbulent transition into account, are used to close the Reynolds equations.

2.1. Basic equations

The equations describing the flow have the following form:

- the equation of continuity

$$\frac{\partial \vartheta_j}{\partial x_j} = 0;$$

- the momentum equation

$$\vartheta_j \frac{\partial \vartheta_i}{\partial x_j} = -\frac{1}{\rho}\frac{\partial p}{\partial x_i} + \frac{\partial}{\partial x_j}\left[(\nu + \nu_t)\frac{\partial \vartheta_i}{\partial x_j}\right];$$

- the energy equation

$$\vartheta_j \frac{\partial T}{\partial x_j} = \frac{\partial}{\partial x_j}\left[\left(\frac{\nu}{\mathrm{Pr}} + \frac{\nu_t}{\mathrm{Pr}_t}\right)\frac{\partial T}{\partial x_j}\right].$$

In this equation, ρ stands for density, ϑ_i for velocity components in the direction of coordinates x_i, p for pressure, T for temperature, ν for the liquid's kinematic viscosity, ν_t for turbulent viscosity, and Pr, Pr_t for the Prandtl number for laminar and turbulent flow regimes. The subsequent equations, which pertain to the turbulence models, are sourced from [26]. For the turbulence model *k*–ε, the dissipation of the turbulent energy ε and the cinematic energy of the turbulence k are determined using the following set of equations:

$$\frac{\partial}{\partial x_i}(\rho k \vartheta_i) = \frac{\partial}{\partial x_j}\left[(\mu + \frac{\mu_t}{\sigma_k})\frac{\partial k}{\partial x_j}\right] + G_k + G_b - \rho\varepsilon - Y_M + S_k$$

$$\frac{\partial}{\partial x_i}(\rho \varepsilon \vartheta_i) = \frac{\partial}{\partial x_j}\left[(\mu + \frac{\mu_t}{\sigma_\varepsilon})\frac{\partial \varepsilon}{\partial x_j}\right] + C_{1\varepsilon}\frac{\varepsilon}{k}(G_k + C_{3\varepsilon}G_b) - C_{2\varepsilon}\rho\frac{\varepsilon^2}{k} + S_\varepsilon.$$

Here ϑ_i is the component of velocity in the corresponding direction, μ is the dynamic viscosity, μ_t is the turbulent viscosity, Y_M is the total dissipation velocity, $G_k, G_b, C_{1\varepsilon}, C_{2\varepsilon}$ are constants, S_k, S_ε are user–defined initial terms.

$$\mu_t = \rho C_\mu \frac{k^2}{\varepsilon}.$$

Additional transfer equations for the k–ω SST model have the form

$$\vartheta_j \frac{\partial Re_{\theta t}}{\partial x_j} = P_{\theta t} + \frac{\partial}{\partial x_j}\left[\sigma_{\theta t}(\nu + \nu_t)\frac{\partial Re_{\theta t}}{\partial x_j}\right];$$

$$\vartheta_j \frac{\partial \gamma}{\partial x_j} = P_\gamma - E_\gamma + \frac{\partial}{\partial x_j}\left[\left(\nu + \frac{\nu_t}{\sigma_\gamma}\right)\frac{\partial \gamma}{\partial x_j}\right];$$

Here $P_{\theta t}$ is a derivative of the Reynolds number in terms of the thickness of the pulse loss; P_γ and E_γ are the conditions for the formation and dissipation of intermittency; $\sigma_{\theta t}$ and σ_γ are the constants of the model, γ is the intermittency parameter.

The traffic sources are defined as follows:

$$P_{\gamma 1} = F_{length} c_{a1} \rho S [\gamma F_{onset}]^{c_{\gamma 3}} (1 - c_{e1}\gamma),$$

where S is the strain rate magnitude; F_{length} is an empirical relation that controls the length of the transition area; F_{onset} is the location of the beginning of the transition, $c_{a1}, c_{e1}, c_{\gamma 3}$ are the constants for the intermittency equation.

The source of destruction/relamination is defined as follows:

$$E_\gamma = c_{a2}\rho\Omega\gamma F_{turb}(c_{e2}\gamma - 1)$$

where Ω is the amount of vorticity, c_{a2}, c_{e2} are constants for the intermittency equation, F_{turb} the function that determines the fracture coefficient outside the laminar boundary layer.

For the Transition SST model, instead of the second equation of the above system, the equation is written

$$\frac{\partial(\rho\vartheta_j\gamma)}{\partial x_j} = P_{\gamma 1} - E_{\gamma 1} + P_{\gamma 2} - E_{\gamma 2} + \frac{\partial}{\partial x_j}\left[(\mu + \frac{\mu_t}{\sigma_\gamma})\frac{\partial \gamma}{\partial x_j}\right].$$

The definitions for $P_{\gamma 1}$, $P_{\gamma 2}$ representing sources of transition, and $E_{\gamma 1}, E_{\gamma 2}$ representing sources of destruction or relamination, are provided below

$$P_{\gamma 1} = c_{a1}F_{length}\rho S[\gamma F_{onset}]^{c_{\gamma 3}},\ P_{\gamma 2} = c_{a2}\rho\Omega\gamma F_{turb}$$

$$E_{\gamma 1} = c_{e1}P_{\gamma 1}\gamma,\ E_{\gamma 2} = c_{e2}P_{\gamma 2}\gamma$$

2.2. Dependence of viscosity on temperature

Unacceptable strains on the pipe walls, "solidification" of the oil, and a halt to pumping can result from a rise in viscosity and the appearance of non-Newtonian qualities with a drop in the temperature of oil pumping. The Walter formula is used in the oil business to determine temperature-dependent kinematic viscosity [3].

$$lg[lg(\nu_1 + \mathrm{c})] = a + blgT$$

where a, b and c are the empirical coefficients characterizing the oil under study, which are located at three experimental points. In this case, for the possibility of applying the Walter formula based on two experimental points, $\mathrm{c} = 0.8$ is often assumed.

The coefficients *a* and *b* in the above formula are from the relations

$$a = \lg[\lg(\nu_1 + 0.8)] - b\lg T$$

$$b = \frac{\lg[\lg(\nu_1 + 0.8)] - \lg[\lg(\nu_2 + 0.8)]}{\lg T_1 - \lg T_2}$$

Here ν_1 and ν_2 are the values of the kinematic viscosity of the liquid at temperatures T_1 and T_2.

2.3. Computational procedure

The values obtained using the logarithmic average temperature pressure method are compared with the results obtained using numerical methods of hydrodynamics. The conditions of stationary and axisymmetric flow are accepted. In calculations, oil is assumed to be a Newtonian liquid with constant density and varying thermophysical parameters. The modeling and calculations were done using the Ansys Fluent program. This is supported, by the consistency and dependability of the flow, which considers mathematical models of physical processes, the discretization of space in CFD, which splits continuous real space and the computational domain into a discrete set of cells that are constant fields and medium properties.

The finite volume method, which enables working with grids of different complexity (unstructured), and the SIMPLE algorithm, which is intended for pressure correction, are the two primary techniques used to discretize the equations. Viscous fluxes are calculated using a centered second-order scheme, whereas inviscid flux components are calculated using the MUSCL scheme. By linking centered second-order finite differences with a dissipative term, the MUSCL scheme, which was founded on conservation principles, ensures the monotonicity of the solution and enhances its spatial accuracy. A flow limiter based on characteristic variables is used to accomplish the alternation between these elements. The resulting system of discrete equations is solved using an effective geometric multigrid approach.

2.4. Coefficients of friction and heat transfer

For the laminar flow regime at Reynolds numbers up to 2320, the coefficient of friction λ was determined by the Poiseuille formula.

$$\lambda = \frac{64}{Re}.$$

Since both laminar and turbulent regimes are possible in the Reynolds number range of 2320 to 4000, no comparison was done in this range. There are no well recognized analytical calculation formulas in the literature, and the experimental points vary significantly. Within the Blasius formula was used to calculate a turbulent flow regime with Reynolds values ranging from 4×10^3 to 10^5.

$$\lambda = \frac{0.31644}{Re^{0.25}}.$$

The Nusselt number is determined by a semi-empirical formula

$$Nu = 0.023\, Re^{0.8}\, Pr^{0.43}.$$

3. Geometry of the tube and heat exchanger

When considering a heat exchanger with a continuously varying temperature of the heat carriers, direct-flow and counter-flow devices are distinguished (Fig.1). Cold oil passes through the central pipe, and the surrounding outer pipe is filled with hot water. The heat exchange process is carried out in such a way that oil moves inside the system through a narrow channel, and a stream of hot water flows around it from the outside, providing the necessary temperature regime. The external surface of the heat exchanger is thermally insulated. In a direct-flow type heat exchanger, hot and cold heat carriers flow in the same direction parallel to each other. In a countercurrent type heat exchanger, two heat carriers flow parallel to each other, but in the opposite direction.

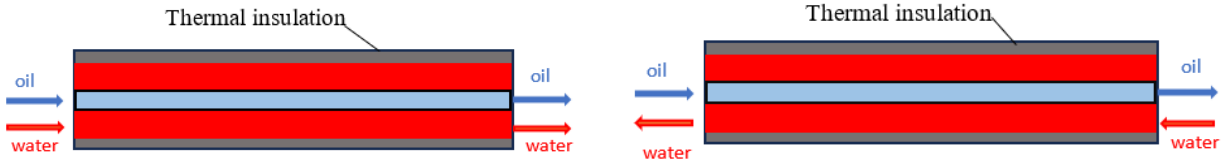

a) b)

Fig. 1. Schemes of direct-flow (a) and counter-flow (b) types of heat exchange devices.

Figure 6 shows the dependences of the Nu number on the Reynolds number (Re) for the cases of smooth and helicode tubes. It can be seen from the figure that for Re numbers up to 2.0×10^4, the heat transfer intensity is higher in the case of a smooth tube than for a helicoid tube. And at values of the Re number above 2.0×10^4, the heat transfer intensity is higher for the helicoid tube. This can be explained by the fact that with this Reynolds number, a laminar-turbulent transition occurs in the flow and it is pronounced precisely in the case of a helicoid tube. The inner diameter of the cold coolant pipe is 12 mm, the outer diameter is 14 mm. The diameter of the pipe through which the hot coolant passes is 20 mm. The temperatures of the heat carriers at the inlet are: cold — 303 K, hot — 423 K. The mass flow rates both of the heat carriers are 0,3814 kg/s and 0,6386 kg/s, respectively, at an inlet flow rate of 4 m/s in each case.

Applying the method of variable viscosity for a cold coolant and offering an improved geometry of the inner tube, in order to comprehensively apply various turbulence models in direct-flow and countercurrent devices, as well as in heat exchangers with a helicoid surface, heat transfer and flow dynamics of coolants are studied taking into account the laminar-turbulent transition. The inner tube of the heat exchanger with a smooth surface is shown in Fig.2a, and a helicoid tube with coils and a design grid is shown in Fig.2b. The number of coils on the surface of the tube is determined by the number of twists N, which in calculations take values from 5 to 40 with an interval of 5 twists.

As part of this task, it is assumed that oil fields are located at a depth of 0.9 to 2.4 km. The density of oil is 844-874 kg/m3, viscosity is 3.4–8.15 MPa·s, sulfur content is 0.16–2%, paraffins are 16-22%, resins are 8-20%. These parameters correspond to the characteristics of the Uzen oil and gas field located in Kazakhstan. These parameters make it possible to accept Uzen oil in the form of a Newtonian fluid [26]. Velocity and temperature profiles corresponding to laminar flow in a circular tube are set as boundary conditions in the inlet section. On the walls of the pipe, sticking conditions are used for speed. In the outlet section of the pipe, mild boundary conditions are applied (zero gradients of the desired functions). Boundary conditions of the second kind are used as boundary conditions for surface temperature.

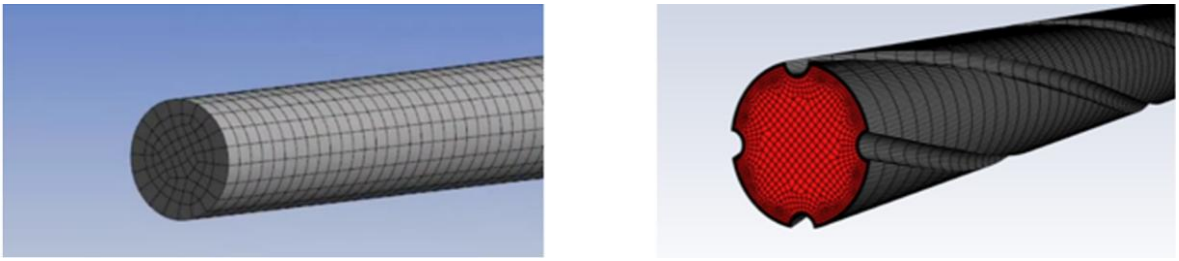

a) b)

Fig. 2. View of smooth (a) and helicoid (b) design tubes.

The calculated grid contains 705,795 nodes and 657,696 elements. When y^+ is the dimensionless wall coordinate, the mesh cells are compressed close to the pipe walls so that $y^+<2$. The following initial parameters of the problem were also used for calculation: the radius of the unicode pipe is $R=0.006$ m, the radius of the groove is $r=0.001$ m, the flow velocity $\vartheta=4$ m/s, the temperature at the pipe inlet $T=303$ K, the heat transfer coefficient $\alpha=16685$ W/(m^2·K). The associated problem of heat exchange and hydrodynamics is solved for the heat exchanger. Boundary conditions of the 3rd kind are used on the walls of pipes. The temperature profiles of water and oil (cold and hot coolants) along the heat exchanger's length were produced using the widely recognized average-logarithmic temperature difference (LMTD) approach, as shown in [26], in order to validate the computation findings.

4. Discussion of the modeling results of flow in the helicoid tube

Based on the calculation results, distributions of hydrodynamic and thermal parameters for smooth and helicoid pipes are obtained. Figure 3a shows a graph of the dependence of the average mass temperature of oil at the outlet of a pipe with a length of 1 m on the number of coils. With an increase in the number of swirls, the oil outlet temperature increases, i.e., heat exchange between the heat carriers intensifies. With a tube length of 1 m, the maximum change in oil outlet temperature is approximately 3 degrees. Data analysis in Fig. 3b demonstrates that the heat flow through the surface of the pipe in contact with the washing liquid increases in proportion to the number of twists. This indicates that a larger number of twists contributes to increased heat transfer.

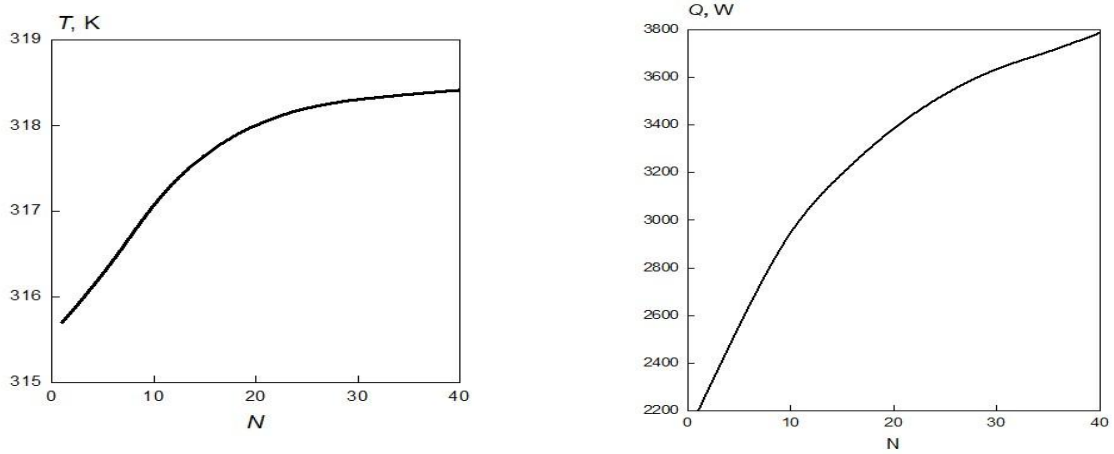

a) b)

Fig. 3. Dependence of the average mass temperature of oil at the outlet of the pipe (a) and heat flow (b) on the number of twists with a pipe length of 1 m.

The observed increase in the average oil temperature at the pipe's output (Fig. 3a) and a rise in heat flow with an increase in the number of twists in the pipe are due to the turbulence of the flow caused by the twisting process itself. The turbulence of the flow enhances the diffusion of liquid particles and, as a result, the intensification of heat exchange between them. The efficiency of this process is directly proportional to the number of twists in the pipe. In further calculations of oil parameters for smooth and helicoid surfaces, the pipe length was assumed to be 4 m, and the number of coils was 40. The data for a smooth pipe are taken from

previous studies [26]. For a helicoid tube, heat exchange occurs more intensively, which is associated with an increase in the surface area of the heat exchange (in the presence of coils), and there is also an increase in heat exchange due to the diffusion process.

Figure 4 shows the dependence of the overpressure along the entire length of the tube. In the case of a helicoid pipe (line 2), a more drastic pressure drop is observed than in the case of a pipe with smooth walls. Additional flow resistance in the helicoid tube is associated with the development of vortex structures and increased friction caused by a violation of the linearity of the flow. Such effects are a consequence of the curved geometry and are accompanied by an increase in hydraulic losses. The coefficient of friction along the pipe was illustrated in Figure 5. It can be seen that the helicoid tube (line 2) exhibits a higher average coefficient of friction than the smooth tube (line 1). The flow and heat exchange in a pipe with spiral grooves are characterized by a number of distinctive features compared to smooth pipes. The presence of spiral grooves on the inner surface of the pipe induces a swirling flow movement, which leads to the formation of stable secondary vortex structures.

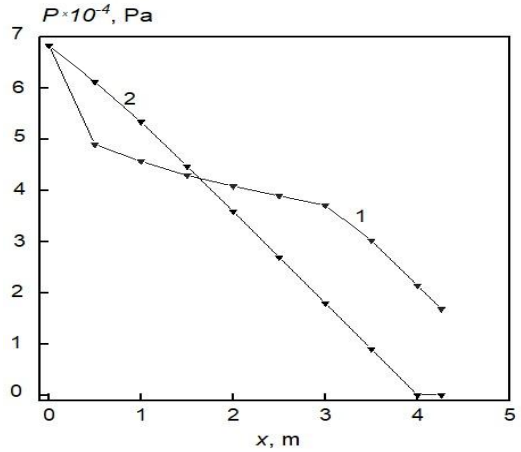

Fig. 4. Changes in oil overpressure along the length of a pipe with a smooth (line 1) and a helicoid (line 2) surface.

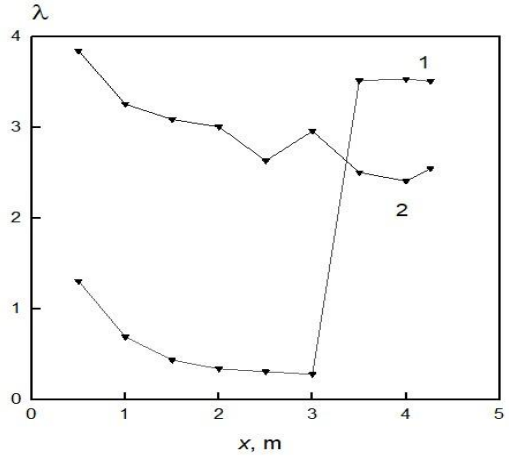

Fig 5. Changes in the coefficient of friction of oil along the length of a pipe with a smooth (line 1) and a helicoid (line 2) surface.

These vortices disrupt the laminar flow structure and contribute to a more uniform temperature distribution across the pipe section. An increase in the level of turbulence is already observed at relatively small values of the Reynolds number, which provides an increase in the intensity of heat transfer between the pipe surface and the moving medium. The grooves create the effect of pseudo-vortex mixtures, enhancing heat transfer and destroying the thermal boundary layer. The flow and heat exchange in a pipe with spiral grooves are characterized by a number of distinctive features compared to smooth pipes. The presence of spiral grooves on the inner surface of the pipe induces a swirling flow movement, which leads to the formation of stable secondary vortex structures. These vortices disrupt the laminar flow structure and contribute to a more uniform temperature distribution across the pipe section. As a result, turbulence increases significantly, even at relatively low values of the Reynolds number, which contributes to the intensification of heat exchange between the pipe wall and the flowing medium. The grooves create the effect of pseudo-vortex mixtures, enhancing heat transfer and destroying the thermal boundary layer. However, along with the increase in heat transfer, there is an increase in hydraulic resistance due to increased friction and vortex formation losses. Thus, the use of pipes with spiral grooves requires optimal design of the geometry of the grooves (depth, pitch, angle of inclination) in order to achieve maximum efficiency with acceptable energy consumption.

Figure 6 shows the dependences of the Nusselt number on the Reynolds number (Re) for the cases of smooth and helicode tubes. It can be seen from the figure that for Re numbers up to 2.0×10^4, the heat transfer intensity is higher in the case of a smooth tube than for a helicoid tube. And at values of the Re number above 2.0×10^4, the heat transfer intensity is higher for the helicoid tube. This can be explained by the fact that with this Reynolds number, a laminar-turbulent transition occurs in the flow and it is pronounced precisely in the case of a helicoid tube.

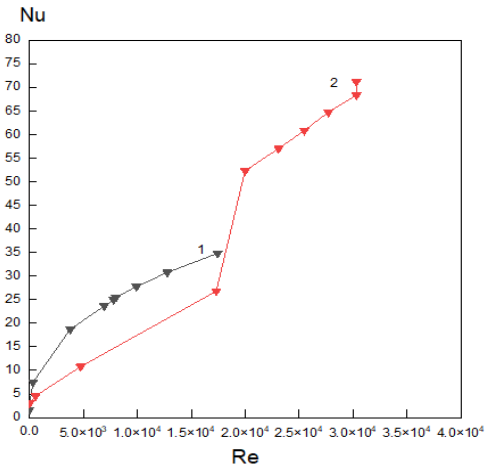

Fig 6. Dependence of the Nusselt number on the Reynolds number for the inner tube with oil. 1 - smooth tube, 2 - helicoid tube.

5. Comparison of the model and experimental analysis of the flow in the heat exchanger

Figures 7 and 8 show changes in the temperature of the heat carriers along the tubes. The graphs are constructed for three turbulence models, covering the forward and countercurrent flow patterns in smooth pipes. Triangular markers indicate calculations performed by the LMTD (Log-Mean Temperature Difference) method [26].

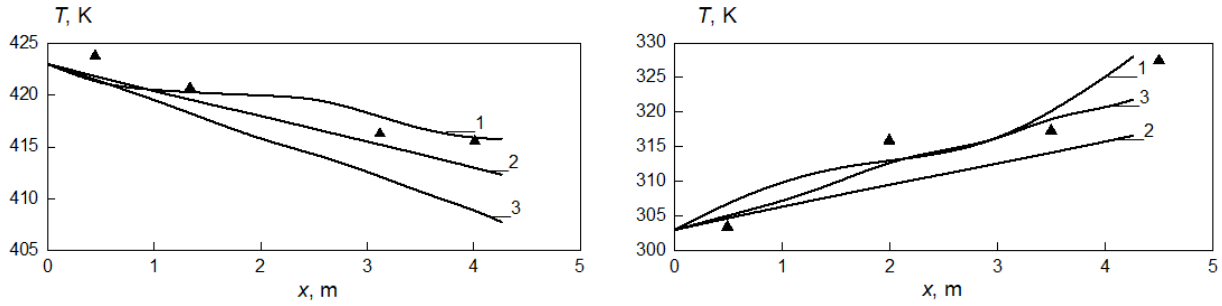

Fig.7. Temperature changes of water (a) and oil (b) along the axial coordinate in a direct–flow heat exchanger for models k–ω SST (lines 1), k-ε (lines 2), Transition SST (lines 3).

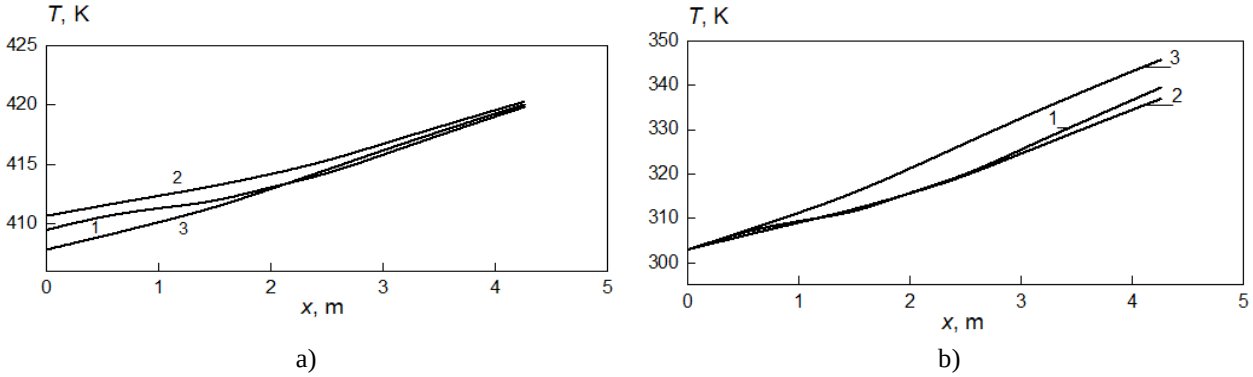

Fig.8. Temperature change of water (a) and oil (b) along the axial coordinate in a countercurrent heat exchanger for models k–ω SST (lines 1), k–ε (lines 2), Transition SST (lines 3).

In the case of direct flow (Fig. 7), all three turbulence models demonstrate a similar pattern of temperature changes: the temperature of the hot coolant (water) decreases, and the temperature of the cold coolant (oil) increases in the axial direction. An analysis of the results shows that for all the turbulence models studied, the

temperature differences between the heat carriers become more pronounced as they approach the outlet section. In particular, the *k–ε* model demonstrates a lower heating temperature of the cold coolant along the pipe compared to the other two models. On the other hand, the most intense cooling of the hot coolant is observed when using the Transition *SST* model. For the counterflow circuit (Fig. 8), the temperature of the cold coolant increases along the pipe in the direction from the inlet section to the outlet for all three turbulence models. However, stronger heating occurs for the Transition SST model compared to the direct-flow case. Unlike direct flow, the flow of hot coolant is directed from the outlet section of the heat exchanger towards its inlet section, therefore, cooling of this coolant occurs from the outlet section towards the inlet section. In this case, cooling occurs more slowly for the *k–ε* model, whereas for the direct current, such a change occurs for the SST model.

A comparison the cold coolants' (oil's) temperature variation for two instances of coolant flow shown in Figures 7 and 8 shows that for the considered turbulence models, the oil heating temperature is higher in the countercurrent case than in the direct-flow scheme with a relatively uniform cooling rate of the hot coolant.

The temperature field in a pipe with grooves is characterized by reduced unevenness compared to a smooth pipe. Due to the intensified mixing, a more efficient destruction of the thermal boundary layer is observed, which leads to a significant increase in the heat transfer coefficient. This effect is especially pronounced in laminar and transient flow regimes, where grooves play the role of an active element of heat exchanger. Figure 9 shows comparative graphs of the calculated and experimental dependences of the Nu number on the Re number for three cases of the turbulence model, namely the *k–ω SST*, *k-ε* and Transition *SST* models. The calculation results were compared with the experimental results in [27, 28]. This experimental work provides an analysis of the thermohydraulic characteristics and energy efficiency of shell-and-tube heat exchangers with a longitudinal flow in a counterflow.

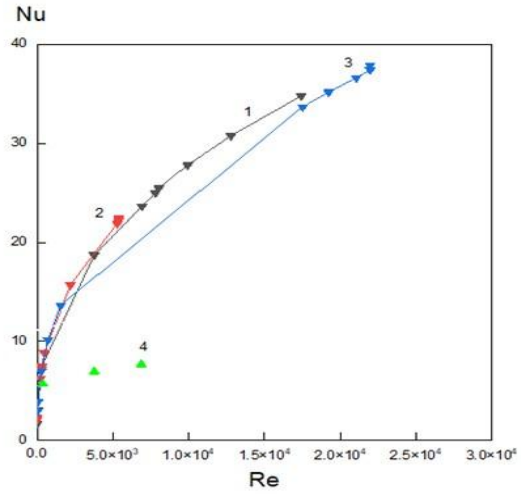

Fig.9. Comparative graphs of the dependences of the numbers Nu and Re in a tube with oil washed by water for all three models and experiment: 1- *k-ω SST*, 2 - *k–ε* model, 3 - Transition *SST* model, 4 - experimental data.

It can be seen from the figure that all three turbulence models give results close to each other, which are qualitatively consistent with the recalculated experimental results (due to different fluid densities). Naturally, one should not expect a quantitative coincidence of the results here, since the Nusselt tabular number for water is an order of magnitude higher than for oil. Nevertheless, the qualitative agreement of the calculated and experimental curves indicates an adequate description of the computational model used in this process.

Despite the physical differences between the cold coolants (water in one case and oil in the other), there is a qualitative agreement between the calculated curve and the experimental one. Naturally, one should not expect a quantitative coincidence of the results here, since the Nusselt table number for water is an order of magnitude higher than for oil. Nevertheless, the qualitative agreement of the calculated and experimental curves indicates an adequate description of the computational model used in this process.

Thus, the presence of spiral grooves makes it possible to significantly increase the efficiency of heat and mass transfer, however, this is accompanied by an increase in energy costs for overcoming resistance. Optimization of the geometry of the grooves (angle of inclination, pitch, depth) allows to achieve the best ratio between the intensification of heat exchange and pressure losses.

***Data Availability Statement*:** The data presented in this study are available upon request from the author.

6. Conclusion

Numerical studies of heat exchange and hydrodynamic characteristics in pipes of various geometries (smooth and helicoid) have revealed a number of fundamental features due to the shape of the channel. The use of a helicoid tube contributes to a significant intensification of heat exchange. The use of swirled tubes with coils leads to a noticeable increase in the oil outlet temperature and the local Nusselt number compared to a smooth pipe. The main reason for this is the turbulence of the oil flow caused by windings, which intensifies the heat exchange between the liquid layers through diffusion. In addition, a slight increase in the surface area of the tube due to the recesses also contributes to an increase in oil temperature, increasing the heat flow. These conclusions are confirmed by comparative graphs of the dependence of the oil outlet temperature for smooth and helical tubes with swirls.

The characteristic behavior of temperature curves is observed for the *k–ε*, *k-ω SST*, and Transition *SST* turbulence models: along the pipe's length, the hot coolant's temperature drops and the cold coolant's temperature rises of the pipe. In the countercurrent mode of movement of heat carriers, intensive heating of oil is observed compared to direct flow, which indicates a higher efficiency of the countercurrent circuit of the heat exchanger. The Transition *SST* model shows the greatest heating of the cold coolant in both modes, while the *k–ε* model demonstrates a smooth and linear behavior of the temperature profile.

In addition, the *k-ω SST* model most effectively identifies the laminar-turbulent transition that occurs in the range of 3-3.5 m from the inlet section and is confirmed by changes in key parameters such as the Reynolds number, heat transfer coefficient and coefficient of friction.

Conflict of interest statement

The authors declare that they have no conflict of interest in relation to this research, whether financial, personal, authorship or otherwise, that could affect the research and its results presented in this paper.

CRediT author statement

Volkov K.N.: Methodology, Conceptualization, Resources; **Jaichibekov N.Zh.:** Supervision, **Calculation** methods, Validation**; Zhumanbayeva A.S.:** Investigation, Data curation, Writing – review & editing; **Kurmanova D.E.:** Visualization, Formal analysis, Writing – original draft. The final manuscript was read and approved by all authors.

Acknowledgments

The authors express their sincere gratitude for the administrative and technical support provided during the implementation of this study: L.N. Gumilyov Eurasian National University and Kingston University (London, UK).

References

1 Kurmanova D.Y., Jaichibekov N.Zh., Karpenko A.G., Volkov K.N. (2023) Numerical modeling and calculation of heat transfer between heat carriers in heat exchangers. *Bulletin of Karaganda University. Physics Series*, 109(1), 59–70. https://doi.org/10.31489/2023ph1/59-70

2 Kurmanova D., Jaichibekov N., Karpenko A., Volkov K. (2023) Modelling and simulation of heat exchanger with strong dependence of oil viscosity on temperature. *Fluids*, 8(95), 1-18. https://doi.org/10.3390/fluids8030095

3 Barilovich V.A., Smirnov Yu.A. (2010) *Fundamentals of technical thermodynamics and theory of heat and mass transfer: a course of lectures*, St.Petersburg, Russia, 338. [in Russian] https://elib.spbstu.ru/dl/1976.pdf/view

4 Karar O., Emani S., Gounder S.M., Myo Thant M.M., Mukhtar H., Sharifpur M., & Sadeghzadeh M. (2021) Experimental and numerical investigation on convective heat transfer in actively heated bundle-pipe. *Engineering Applications of Computational Fluid Mechanics*, 15(1), 848-864. https://doi.org/10.1080/19942060.2021.1920466

5 Rana S., Zunaid M., Kumar R. (2022) CFD approach for the enhancement of thermal energy storage in phase change material charged heat exchanger. *Case Studies in Thermal Engineering*, 33, 101921. https://doi.org/10.1016/j.csite.2022.101921

6 Borse D., Bute J.V. (2018) A review on helical coil heat exchanger. *International Journal for Research in Applied Science and Engineering Technology*, 6, 492–497. https://doi.org/10.22214/ijraset.2018.2070

7 Inyang U., Uwa I. (2022) Heat transfer in helical coil heat exchanger. *Advances in Chemical Engineering and Science*, 12, 26–39. https://doi.org/10.4236/aces.2022.121003

8 Marzouk S.A., Al-Sood M.M., El-Said M.S., Younes M.M., & El Fakharany M.K. (2023) A comprehensive review of methods of heat transfer enhancement in shell and tube heat exchangers. *Journal of Thermal Analysis and Calorimetry*, 148, 7539–7578. https://doi.org/10.1007/s10973-023-12265-3

9 Coronel P, Sandeep K.P. (2008) Heat transfer coefficient in helical heat Exchangers under turbulent flow conditions. *International Journal of Food Engineering*, 4(1). https://doi.org/10.2202/1556-3758.1209

10 Inyang U., Uwa I. (2022) Heat transfer in helical coil heat exchanger. *Advances in Chemical Engineering and Science*, 12, 26–39. https://doi.org/10.4236/aces.2022.121003

11 Jayakumar J.S., Mahajani S.M., Mandal J.C., Vijayan P.K., & Bhoi R. (2008) Experimental and CFD estimation of heat transfer in helically coiled heat exchangers. *Chemical Engineering Research and Design*, 86(3), 221–232. https://doi.org/10.1016/j.applthermaleng.2016.04.037

12 Reddy N.S., Vishwanath K.C., Satheesha V., Thejaraju R., Raj K.N., Manoj M., Goutham H., & Manjunatha B.S. (2021) Study on heat transfer and pressure drop in tube-in-tube helical heat exchanger. *Journal of Applied Science and Engineering*, 24(4), 635–642. https://doi.org/10.6180/jase.202108_24(4).0019

13 Prabhanjan D.G., Raghavan G.S.V., Rennie T.J. (2002) Comparison of heat transfer rates between a straight tube heat exchanger and a helically coiled heat exchanger. *International Communications in Heat and Mass Transfer*, 29(2), 185–191. https://doi.org/10.1016/S0735-1933(02)00309-3

14 Liu Y., Rao Y., Weigand B. (2019) Heat transfer and pressure loss characteristics in a swirl cooling tube with dimples on the tube inner surface. *International Journal of Heat and Mass Transfer*, 128(2), 54–65. https://doi.org/10.1016/j.ijheatmasstransfer.2018.08.097

15 Kurnia J.C., Sasmito A.P., Shamim T., Mujumdar A.S. (2016) Numerical investigation of heat transfer and entropy generation of laminar flow in helical tubes with various cross sections. *Applied Thermal Engineering*, 102, 849–860. https://doi.org/10.1016/j.applthermaleng.2016.04.037

16 Eliseev V.V., Vetyukov Yu.M., Zinovieva T.V. (2011) Divergence of a helicoidal shell in a pipe with flowing liquid. *Journal of Applied Mechanics and Technical Physics*, 52, 450–458. https://doi.org/10.1134/S002189 4411030151

17 Morales R.E., Rosa E.S. (2007) Modeling of free surface flow in a helical channel with finite pitch. *Journal of the Brazilian Society of Mechanical Sciences and Engineering*, 29, 345–353. https://doi.org/10.1590/S16785878200700040002

18 Kelbaliev G.I., Rasulov S.R., Rzaev A.G., Mustafaeva G.R. (2017) Rheology of structured oils. *Journal of Engineering Physics and Thermophysics*, 90, 996–1002. https://doi.org/10.1007/s10891-017-1649-z

19 Yogesh S.S., Selvaraj A.S., Ravi D.K., Rajagopal T.K.R. (2018) Heat transfer and pressure drop characteristics of inclined elliptical fin tube heat exchanger of varying ellipticity ratio using CFD code. *International Journal of Heat and Mass Transfer*, 119, 26–39. https://doi.org/10.1016/j.ijheatmasstransfer.2017.11.094

20 Allouche,Y., Varga S., Bouden C., Oliveira A.C. (2016) Validation of a CFD model for the simulation of heat transfer in a tubes-in-tank PCM storage unit. *Renewable Energy*, 89, 371–379. https://doi.org/10.1016/j.renene.2015.12.038

21 Balaji D., Prakash L.S.S. (2016) CFD analysis of a pressure drop in a staggered tube bundle for a turbulent cross flow. *International Advanced Research Journal in Science, Engineering and Technology*, 3(2), 35–40. https://iarjset.com/upload/2016/february-16/IARJSET%209.pdf

22 Volkov K.N., Emelaynov V.N. (2012) *Computational technologies in problems of fluid and gas mechanics.* Moscow, 468. [in Russian] https://books.google.kz/books/about/%D0%92%D1%

23 Chen K., Mohammed H.I., Mahdi J.M., Rahbari A., Cairns A., & Talebizadehsardari P. (2022) Effects of non-uniform fin arrangement and size on the thermal response of a vertical latent heat triple-tube heat exchanger. *Journal of Energy Storage*, 45, 103723. https://doi.org/10.1016/j.est.2021.103723

24 Czarnota T., Wagner C. (2016) Turbulent convection and thermal radiation in a cuboidal Rayleigh–Binard cell with conductive plates. *International Journal of Heat and Fluid Flow*, 57, 150–172. https://doi.org/10.1016/j.ijheatfluidflow.2015.10.006

25 Mohanan A.K., Prasad B.V., Vengadesan S. (2020) Flow and heat transfer characteristics of a cross-flow heat exchanger with elliptical tubes. *Heat Transfer Engineering*, 42(21), 1–15. https://doi.org/10.1080/01457632.2020.1826742

26 Sakipova S.E., Shaimerdenova K.M., Nussupbekov B.R., Ospanova D.A., Kutum B.B. (2023) Modeling the dynamics of heat and mass transfer processes in a tubular heat exchanger under pulsed influences. *Eurasian Physical Technical Journal*, 1(43), 51-55. https://doi.org/10.31489/2023No1/51-55

27 Erik Dick, Slawomir Kubacki. (2017) Transition Models for Turbomachinery Boundary Layer Flows: A Review. *International Journal of Turbomachinery, Propulsion and Power*, 2(2), 1-45. https://doi.org/10.3390/ijtpp2020004

28 Niangi Li, Jian Chen, Tao Cheng, Jiří Jaromír Klemeš, Petar Sabev Varbanov, Qiuwang Wang, Weisheng Yang, Xia Liu, Min Zeng (2020) Analysing thermal-hydraulic performance and energy efficiency of shell-and-tube heat exchangers with longitudinal flow based on experiment and numerical simulation. *Energy*, 202, 117757. https://doi.org/10.1016/j.energy.2020.117757

AUTHORS' INFORMATION

Zhumanbayeva, Aizhan Serikovna – Doctoral graduate, Senior lecturer, Faculty of Mechanics and Mathematics, L.N. Gumilyov Eurasian National University, Astana, Kazakhstan; Scopus Author ID: 59328973500; https://orcid.org/0009-0007-2725-3672l; jas968@mail.ru

Volkov, Konstantin Nikolaevich – Doctor of Physical and Mathematical Sciences, Senior lecturer, Faculty of Science, Engineering and Computing, Kingston University, London, UK; Scopus Author ID: 8663950000; https://orcid.org/0000-0001-6055-2323; k.volkov@kingston.ac.uk

Jaichibekov Nurbulat Zhumabekovich – Doctor of Physical and Mathematical Sciences, Professor, Faculty of Mechanics and Mathematics, L.N. Gumilyov Eurasian National University, Astana, Kazakhstan; Scopus Author ID: 57195809348; WoS Researcher ID: A-2780-2015 ; https://orcid.org/0000-0002-3053-8288; jaich@mail.ru

Kurmanova Dinara Esentayevna – Ph.D, Senior lecturer, Faculty of Mechanics and Mathematics, L.N. Gumilyov Eurasian National University, Astana, Kazakhstan; Scopus Author ID: 58163166200; https://orcid.org/0009 0009-9787-7426; dikonya89_29@mail.ru